The Journal of Experimental Biology 214, 3630-3638

doi:10.1242/jeb.057406

RESEARCH ARTICLE

Identification and functional characterization of an ovarian aquaporin from the cockroach *Blattella germanica* L. (Dictyoptera, Blattellidae)

Alba Herraiz[1], François Chauvigné[2], Joan Cerdà[2], Xavier Bellés and Maria-Dolors Piulachs[1,*]

[1]Institut de Biologia Evolutiva (CSIC-UPF) and LINC-Global, Passeig Marítim de la Barceloneta 37-49, 08003 Barcelona, Spain and [2]Laboratory of Institut de Recerca i Tecnologia Agroalimentàries (IRTA)–Institut de Ciències del Mar (CSIC), Passeig Marítim de la Barceloneta 37-49, 08003 Barcelona, Spain

*Author for correspondence (mdolors.piulachs@ibe.upf-csic.es)

Accepted 8 August 2011

SUMMARY

Aquaporins (AQPs) are membrane proteins that form water channels, allowing rapid movement of water across cell membranes. AQPs have been reported in species of all life kingdoms and in almost all tissues, but little is known about them in insects. Our purpose was to explore the occurrence of AQPs in the ovary of the phylogenetically basal insect *Blattella germanica* (L.) and to study their possible role in fluid homeostasis during oogenesis. We isolated an ovarian AQP from *B. germanica* (BgAQP) that has a deduced amino acid sequence showing six potential transmembrane domains, two NPA motifs and an ar/R constriction region, which are typical features of the AQP family. Phylogenetic analyses indicated that BgAQP belongs to the PRIP group of insect AQPs, previously suggested to be water specific. However, ectopic expression of BgAQP in *Xenopus laevis* oocytes demonstrated that this AQP transports water and modest amounts of urea, but not glycerol, which suggests that the PRIP group of insect AQPs may have heterogeneous solute preferences. BgAQP was shown to be highly expressed in the ovary, followed by the fat body and muscle tissues, but water stress did not significantly modify the ovarian expression levels. RNA interference (RNAi) reduced BgAQP mRNA levels in the ovary but the oocytes developed normally. The absence of an apparent ovarian phenotype after BgAQP RNAi suggests that other functionally redundant AQPs that were not silenced in our experiments might exist in the ovary of *B. germanica*.

Supplementary material available online at http://jeb.biologists.org/cgi/content/full/214/21/3630/DC1

Key words: BgAQP, water channel, urea transport, drought, oogenesis, panoistic ovary, insect, *Drosophila*.

INTRODUCTION

Aquaporins (AQPs) are membrane proteins that facilitate water transport, and have been identified from species belonging to all life kingdoms, including unicellular (archaea, bacteria, yeast and protozoa) and multicellular (plants and animals) organisms (King et al., 2004; Maurel et al., 2008). They belong to the major intrinsic proteins (MIP) superfamily that share a common structure comprising six transmembrane domains (TM1–TM6) connected by five loops (A–E), and cytoplasmic N- and C-termini. AQPs contain two canonical Asp–Pro–Ala (NPA) motifs located in steric contiguity with the aromatic/arginine (ar/R) constriction region involved in proton exclusion and channel selectivity (de Groot et al., 2003; Murata et al., 2000). The ar/R constriction site is defined by four residue positions (56, 180, 189 and 195; human AQP1 numbering), which in water-selective AQPs are Phe^{56}, His^{180}, Cys^{189} and Arg^{195} (human AQP1) (de Groot et al., 2003). The AQP polypeptide chain is formed by two closely related halves that may have arisen by gene duplication (Zardoya, 2005). In the cell membrane, each AQP is folded into a right-handed α-barrel, with a central transmembrane channel surrounded by the six full-length transmembrane helices and the two NPA-containing loops, B and E. This conformation in the plasma membrane is known as the hourglass model (Jung et al., 1994). Some AQPs, known as aquaglyceroporins, transport other non-charged solutes such as glycerol and urea in addition to water (Gomes et al., 2009; Rojek et al., 2008; Törnroth-Horsefield et al., 2010). The amino acids forming the ar/R constriction (His is replaced by the smaller amino acid Gly in aquaglyceroporins) (Beitz et al., 2006), and five other residues (P1–P5) located on the side-chains neighbouring the ar/R constriction (Froger et al., 1998), are responsible for substrate selectivity. The transport function of many AQPs is inhibited by mercurial sulfhydryl-reactive compounds, such as $HgCl_2$, which block the water pore (Hirano et al., 2010; Preston et al., 1993).

While there are considerable data on mammalian AQPs, studies on insect AQPs are much more limited. Phylogenetic analysis based on 18 insect genomes revealed the presence of AQP orthologues in all of them (Campbell et al., 2008). However, only 15 AQPs from insects have been characterized in terms of substrate selectivity (Campbell et al., 2008; Goto et al., 2011; Kataoka et al., 2009a; Kataoka et al., 2009b; Liu et al., 2011; Philip et al., 2011). The first insect AQP to be functionally characterized was AQPcic, from the filter chamber of *Cicadella viridis*, and was shown to be water selective (Le Caherec et al., 1996). Since then, water-transporting AQPs have also been isolated from *Aedes aegypti* (Duchesne et al., 2003), *Rhodnius prolixus* (Echevarria et al., 2001), *Drosophila melanogaster* (Kaufmann et al., 2005), *Polypedilum vanderplanki* (Kikawada et al., 2008), *Acyrthosiphon pisum* (Shakesby et al., 2009), *Bombyx mori* (Kataoka et al., 2009a), *Grapholita molesta* (Kataoka et al., 2009b), *Eurosta solidaginis* (Philip et al., 2011), *Anopheles gambiae* (Liu et al., 2011) and *Belgica antarctica* (Goto

et al., 2011). Only two insect AQPs have been shown to transport glycerol and urea in addition to water: AQP-Bom2 and AQP-Gra2, from *B. mori* and *G. molesta*, respectively (Kataoka et al., 2009a; Kataoka et al., 2009b). Finally, *D. melanogaster* Big Brain AQP transports monovalent cations in the epidermal precursor regions of developing larvae (Yanochko and Yool, 2002).

Our aim was to investigate the presence of AQPs in the ovary of the cockroach *Blattella germanica* (Dictyoptera, Blattellidae) and their possible role in water homeostasis during oogenesis and vitellogenesis. *Blattella germanica* has panoistic ovaries, which is the less modified insect ovarian type (Büning, 1994). During oocyte maturation, basal oocytes increase in size through the incorporation of vitellogenin, other yolk precursors and water (Belles et al., 1987; Ciudad et al., 2006; Martín et al., 1995; Telfer, 2009). Moreover, although *B. germanica* is well adapted to xeric environments (Appel, 1995), water stress readily leads to oocyte resorption. These circumstances make *B. germanica* a good model for studying ovarian AQPs. Finally, insect AQPs that have been described so far were from holometabolans or phylogenetically distal hemimetabolans (hemipterans and phthirapterans, within the paraneopterans), and therefore *B. germanica*, which is a phylogenetically basal insect within the polyneopterans, is of evolutionary interest.

MATERIALS AND METHODS

Insects

Female specimens of *B. germanica* were used in all experiments. They were obtained from a colony reared in the dark at 30±1°C and 60–70% relative humidity in a non-aseptic environment. Under these conditions, the cockroach fat body and ovary harbour the endosymbiont bacteroid *Blattabacterium cuenoti* (Giorgi and Nordin, 1994; Lopez-Sanchez et al., 2009). Sixth instar nymphs or freshly ecdysed adult females were selected from the colony and used at appropriate ages. All dissections and tissue sampling were carried out on carbon dioxide-anaesthetized specimens. Tissues used in the experiments were as follows: entire ovary, fat body abdominal lobes, levator and depressor muscles of tibia, digestive tract from the pharynx to the rectum (Malphigian tubules excluded), isolated Malpighian tubules and colleterial glands. After the dissection, the tissues were frozen in liquid nitrogen and stored at –80°C until use.

Cloning and sequencing

The sequence of a partial cDNA encoding a putative *B. germanica* AQP (544 bp) was obtained from an expressed sequence tag (EST) library available in GenBank (accession number FG128078.1). This fragment was amplified from cDNA synthesized from 3 day old adult ovaries using specific oligonucleotide primers and conventional RT-PCR. The resulting fragment was cloned into pSTBlue-1 vector (Novagen, Madrid, Spain) and sequenced. To clone the full-length cDNA, 5′- and 3′-RACE (Invitrogen, Paisley, UK) were used according to the manufacturer's instructions. The PCR products were analysed by agarose gel electrophoresis, cloned into pSTBlue-1 vector and sequenced. The sequence, which proved to be an AQP homologue, was named BgAQP (accession number FR744897).

Comparison of sequences and phylogenetic analysis

Putative insect AQP sequences were retrieved from GenBank. Protein sequences were aligned with that obtained for *B. germanica*, using CLUSTALX (v 1.83). Poorly aligned positions and divergent regions were removed using GBLOCKS 0.91b (http://molevol.cmima.csic.es/castresana/Gblocks.html) (Castresana, 2000). The resulting alignment was analysed by the PHYML 3.0 program (Guindon and Gascuel, 2003) based on the maximum-likelihood principle with the amino acid substitution model. The data were bootstrapped for 100 replicates using PHYML. The sequences used in the phylogenetic analysis were as follows. XP_002429480.1 (*Pediculus humanus*), AAL09065.1 (PrAQP1, *Pyrocoelia rufa*), FJ489680 (*Es*AQP1, *E. solidaginis*), NP_610686.1 (DmPRIP, *D. melanogaster*), XP_001865728.1 (*Culex quinquefasciatus*), XP_001656932.1 (AaAQP2, *A. aegypti*), BAF62090.1 (PvAQP1, *P. vanderplanki*), AB602340 (BaAQP1, *B. antarctica*), XP_319585.4 (AgAQP1, *A. gambiae*), NP_001153661.1 (*B. mori*), XP_968342.1 (TcPRIP, *Tribolium castaneum*), XP_001607929.1 (NvPRIP, *Nasonia vitripennis*), XP_394391.1 (*Apis mellifera*), XP_972862.1 (TcDRIP, *T. castaneum*), Q23808.1 (AQPcic, *C. viridis*), BAG72254.1 (*Coptotermes formosanus*), XP_002425393.1 (*P. humanus*), ABW96354.1 (*Bemisia tabaci*), XP_624531.1 (AmDRIP, *A. mellifera*), (NvDRIP, *N. vitripennis*), AAA81324.1 (DmDRIP, *D. melanogaster*), AAA96783.1 (BfWC1, *Haematobia irritans*), ABV60346.1 (LlAQP, *Lutzomyia longipalpis*), XP_319584.4 (*A. gambiae*), AF218314.1 (AaAQP1, *A. aegypti*), XP_001865732.1 (*C. quinquefasciatus*), BAD69569.1 (AQP-Bom1, *B. mori*), BAH47554.1 (AQP-Gra1, *G. molesta*), NP_001139376.1 (*A. pisum*), NP_001139377.1 (*A. pisum*), XP_396705.2 (AmBIB, *A. mellifera*), XP_001604170.1 (NvBIB *N. vitripennis*), XP_314890.4 (*A. gambiae*), XP_001649747.1 (AaAQP3, *A. aegypti*), XP_001866597.1 (*C. quinquefasciatus*), XP_314891.4 (*A. gambiae*), AAF52844.1 (DmBIB, *D. melanogaster*), XP_968782.1 (TcBIB, *T. castaneum*), XP_970791.1 (*T. castaneum*), XP_970912.1 (*T. castaneum*), XP_001121899.1 (*A. mellifera*), XP_001601231.1 (*N. vitripennis*), XP_624194.1 (*A. mellifera*), XP_001601253.1 (*N. vitripennis*), NP_001106228.1 (AQP-Bom2, *B. mori*), BAH47555.1 (AQP-Gra2, *G. molesta*), BAF62091.1 (PvAQP2, *P. vanderplanki*), XP_001650169.1 (AaAQP5, *A. aegypti*), XP_001850887.1 (*C. quinquefasciatus*), XP_318238.4 (*A. gambiae*), NP_611812.1 (*D. melanogaster*), NP_611813.1 (*D. melanogaster*), NP_611811.3 (*D. melanogaster*), XP_001650168.1 (AaAQP4, *A. aegypti*), XP_554502.2 (*A. gambiae*), NP_611810.1 (*D. melanogaster*), XP_001121043.1 (*A. mellifera*), XP_001603421.1 (*N. vitripennis*) and XP_970728.1 (*T. castaneum*).

Structural predictions

Topographical analyses to determine transmembrane regions were carried out with the programs TMHMM (www.cbs.dtu.dk/services/TMHMM/) (Krogh et al., 2001) and SMART (http://smart.embl-heidelberg.de/smart/set_mode.cgi) (Letunic et al., 2009). Phosphorylation sites and kinases were determined using NetPhos 2.0 and NetPhosK 1.0 programs (Blom et al., 1999; Blom et al., 2004), respectively, on ExPASy Proteomic Tools (http://expasy.org/tools). Predictions of tridimensional structure were carried out with the 3D-JIGSAW Protein Comparative Modelling Server (http://bmm.cancerresearchuk.org/~3djigsaw/) (Bates et al., 2001), and analysed using PyMOL Molecular Graphics System (version 1.2r3pre, Schrödinger, LLC).

Functional expression in *Xenopus laevis* oocytes

The open reading frame (ORF) of BgAQP cDNA was cloned into the pSTBlue-1 vector and subcloned into the *Eco*RV/*Spe*I sites of the pT7Ts expression vector (Deen et al., 1994). Capped RNA (cRNA) was synthesized *in vitro* with T7 RNA polymerase (Roche, Barcelona, Spain) from *Xba*I-linearized pT7Ts vector containing the BgAQP cDNA. The isolation and microinjection of stage V–VI oocytes of *X. laevis* was carried out as previously described (Deen

et al., 1994). For water permeability experiments, oocytes were injected with either 50 nl of RNase-free water (negative control) or 50 nl of water containing 10 ng BgAQP cRNA. For glycerol and urea uptake experiments, oocytes were injected with 25 ng of BgAQP, human AQP1 (negative control) or human AQP3 (positive control) cRNA. Human AQP1 and AQP3 were kindly provided by P. Deen (Department of Physiology, Radboud University Nijmegen Medical Centre, Nijmegen, The Netherlands).

Swelling assays

Osmotic water permeability (P_f) was measured from the time course of oocyte swelling in a standard assay (Deen et al., 1994). Water- and cRNA-injected *X. laevis* oocytes were transferred from 200 mOsm modified Barth's culture medium [MBS; 0.33 mmol l^{-1} $Ca(NO_3)_2$, 0.4 mmol l^{-1} $CaCl_2$, 88 mmol l^{-1} NaCl, 1 mmol l^{-1} KCl, 2.4 mmol l^{-1} $NaHCO_3$, 10 mmol l^{-1} Hepes, 0.82 mmol l^{-1} $MgSO_4$, pH 7.5] to 20 mOsm MBS at room temperature. Oocyte swelling was followed by video microscopy using serial images at 2 s intervals during the first 20 s period. The P_f values were calculated taking into account the time course changes in relative oocyte volume [$d(V/V_o)/dt$], the molar volume of water (V_w=18 cm^3 ml^{-1}) and the oocyte surface area (S), using the formula $V_o[d(V/V_o)/dt]/[SV_w(Osm_{in}–Osm_{out})]$. To examine the inhibitory effect of mercury on P_f, oocytes were pre-incubated for 15 min in MBS containing 1 mmol l^{-1} $HgCl_2$ before and during the swelling assays. To determine the reversibility of the inhibition, the oocytes were rinsed twice with fresh MBS and incubated for another 15 min with 5 mmol l^{-1} β-mercaptoethanol before being subjected to swelling assays.

Radioactive solute uptake assays

To determine the uptake of [^{3}H]glycerol (60 Ci mmol l^{-1}) and [^{14}C]urea (52 mCi mmol l^{-1}), groups of 10 *X. laevis* oocytes injected with water or 25 ng cRNA encoding BgAQP, human AQP1 or human AQP3 were incubated in 200 µl of MBS containing 20 µCi of the radiolabelled solute (cold solute was added to give 1 mmol l^{-1} final concentration) at room temperature. After 10 min (including zero time for subtraction of the signal from externally bound solute), oocytes were washed rapidly 3 times in ice-cold MBS, and individual oocytes were dissolved in 10% SDS for 1 h before scintillation counting.

RNA extraction and reverse transcription to cDNA

All RNA extractions were performed using the Gen Elute Mammalian Total RNA kit (Sigma, Madrid, Spain). A 400 ng sample from each RNA extraction was DNase treated (Promega, Madison, WI, USA) and reverse transcribed with Superscript II reverse transcriptase (Invitrogen, Carlsbad, CA, USA) and random hexamers (Promega). RNA quantity and quality were estimated by spectrophotometric absorption at 260 nm in a Nanodrop Spectrophotometer ND-1000® (NanoDrop Technologies, Wilmington, DE, USA).

Determination of mRNA levels with quantitative real-time PCR

Quantitative real-time PCR (qRT-PCR) reactions were carried out in triplicate in an iQ5 Real-Time PCR Detection System (Bio-Rad Laboratories, Hercules, CA, USA), using IQ™ SYBR Green Supermix (BioRad). A control without template was included in all batches. The efficiency of each primer set was first validated by constructing a standard curve using four serial dilutions. The PCR program began with a single cycle at 95°C for 3 min, followed by 40 cycles at 95°C for 10 s and 55°C for 30 s. mRNA levels were calculated relative to BgActin-5c (GenBank accession number AJ862721) expression, using Bio-Rad iQ5 Standard Edition Optical System Software (version 2.0). The results are given as copies of mRNA per 1000 copies of BgActin-5c mRNA.

Induction of water stress

In order to identify the point at which water stress causes clear phenotypical effects, adult *B. germanica* females were initially subjected to water deprivation from day 0, 1, 3 or 4. All specimens that were water deprived from day 0 and day 1 died after 8–11 days, whereas those water deprived from day 4 did not present any phenotype. Specimens that were water deprived from day 3 showed ovarian resorption starting on day 5. Thus, we decided to follow this treatment, in comparison with a control group that received water *ad libitum*. Water-deprived and control specimens were studied at 24 h intervals until day 7 of adult life.

RNAi experiments

A dsRNA (dsBgAQP) was prepared encompassing a 188 bp region starting at nucleotide 771 of the BgAQP sequence. The fragment was amplified by PCR and cloned into the pSTBlue-1 vector. As control dsRNA (dsMock), we used a 307 bp sequence from *Autographa californica* nucleopolyhedrovirus (GenBank accession number K01149, nucleotides 370–676). The preparation of the dsRNAs was performed as previously described (Ciudad et al., 2006). Freshly emerged specimens from the last (6th) nymphal instar were injected into the abdomen with 3 µg of dsBgAQP in a volume of 1 µl. Control specimens were injected with the same volume and dose of dsMock. After the imaginal moult, one mature male (6–8 days old) per female was added to the rearing jars, in order to bring about mating.

Statistics

Data are expressed as means ± s.e.m. Statistical analysis of gene expression values was carried out using the REST-2008 program [Relative Expression Software Tool V 2.0.7; Corbett Research (Pfaffl et al., 2002)]. This program calculates changes in gene expression between two groups, control and sample, using the corresponding distributions of Ct values as input. Values of P_f and radioactive solute uptake were statistically analysed by Student's unpaired t-test.

RESULTS

Cloning and sequence characterization of BgAQP from *B. germanica*

The sequence of a partial cDNA encoding a *B. germanica* AQP was cloned from ovarian tissue of 3 day old adult females using specific primers based on an EST deposited in GenBank (accession number FG128078.1). This EST nucleotide sequence was derived from male and female whole organisms. Consecutive 5′- and 3′-RACE experiments were carried out in order to obtain the full-length cDNA, which was named BgAQP (GenBank accession number FR744897). The BgAQP cDNA is 1838 bp long and contains an ORF encoding a polypeptide of 277 amino acids (nucleotide positions 95–925) with an estimated molecular mass of 29,541 Da and an isoelectric point of 5.86 (supplementary material Fig. S1). Hydrophobicity and tridimensional predictions indicate that BgAQP has six putative transmembrane domains, five connecting loops, and cytoplasmic N- and C-termini, which are typical AQP features. The second (B) and fifth (E) loops contain the highly conserved NPA motifs (residues 93–95 and 209–211). The amino acids forming the ar/R constriction region (Phe^{73}, His^{197} and Arg^{212}) and the P1–P5 residues (Thr^{133}, Thr^{213}, Ala^{217}, Tyr^{229} and Trp^{230}), which are conserved in water-selective AQPs, are present in BgAQP. In the

amino acid sequence, a consensus motif for *N*-linked glycosylation [NX(S/T)] in loop C (Asn^{35}), as well as seven potential phosphorylation sites (Thr^{48}, Thr^{53}, Ser^{207}, Ser^{220}, Thr^{255}, Thr^{257} and Ser^{260}) and one protein kinase C-specific site (Ser^{216}), were also identified (supplementary material Fig. S1).

Phylogenetic analysis of BgAQP

As the fat body and the ovary of *B. germanica* harbour the endosymbiont bacteroid *B. cuenoti* (Giorgi and Nordin, 1994), we first evaluated whether the putative AQP cDNA cloned really originated from the host cockroach ovary. BLAST analyses against the genome of *B. cuenoti* (Lopez-Sanchez et al., 2009) revealed that the bacteroid does not have any gene sequence matching the nucleotide sequence of BgAQP, which indicates that the cloned cDNA must have come from *B. germanica*. Next, in order to place BgAQP in an evolutionary context within insects, we carried out a phylogenetic analysis of representative insect AQPs available in public databases. The amino acid alignment of these sequences suggested that BgAQP was most closely related to a putative AQP from the phthirapteran *P. humanus* (XP_002429480) and the AQP homologue from the coleopteran *P. rufa* (AAL09065.1). Subsequently, following maximum-likelihood analyses, we obtained the tree depicted in Fig. 1. This tree shows the same general topology published by Campbell and colleagues (Campbell et al., 2008) and more recently by Mathew and colleagues (Mathew et al., 2011), who defined four main clusters of insect AQPs: PRIP (*P. rufa* integral protein), DRIP (*Drosophila* integral protein), BIB (neurogenic gene *Drosophila* big brain) and a fourth cluster of unclassified AQPs. In our tree, BgAQP falls into the well-supported (96% bootstrap value) PRIP cluster, whereas the DRIP cluster

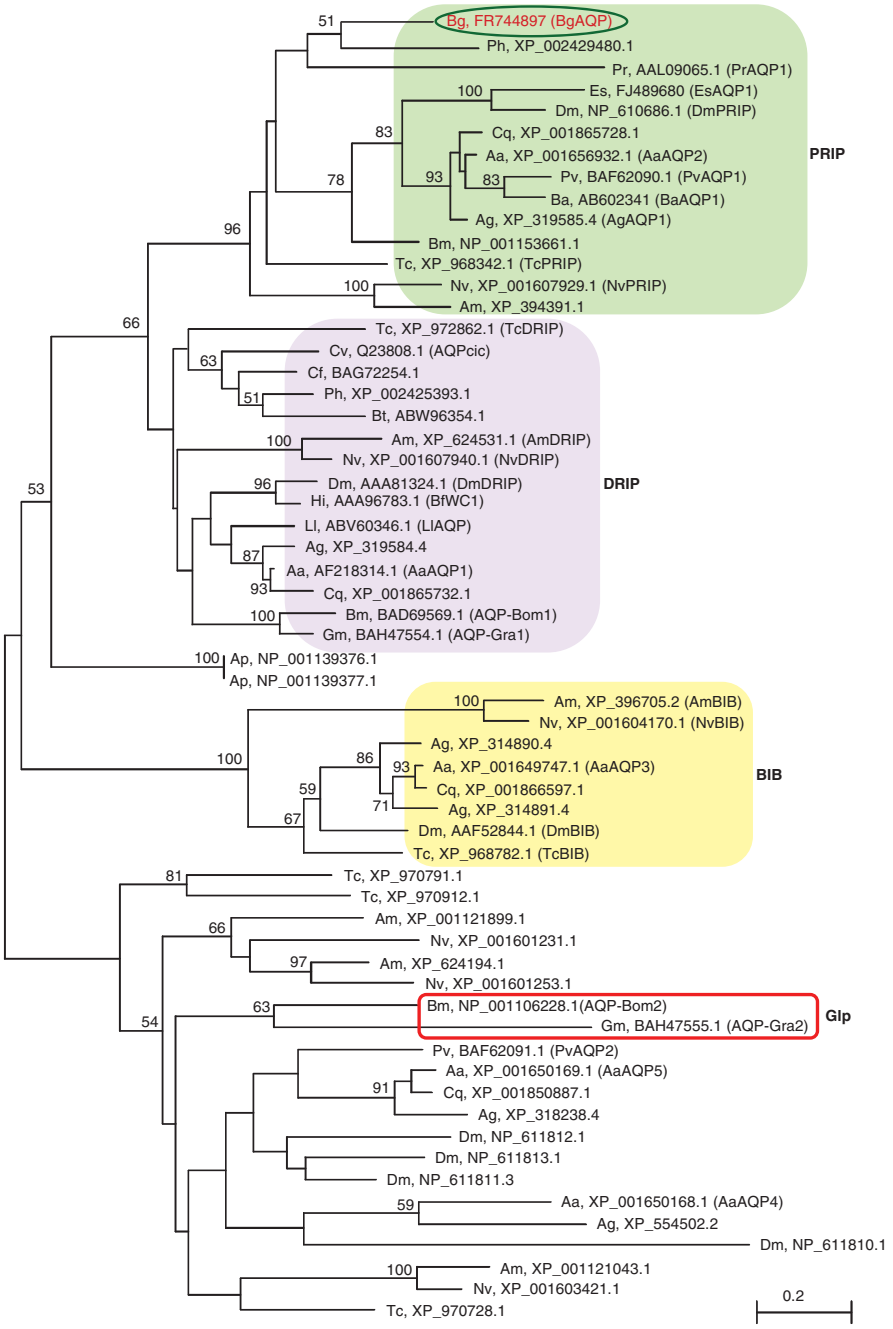

Fig. 1. Maximum-likelihood phylogenetic tree showing the position of *Blattella germanica* aquaporin (BgAQP, ringed) with respect to other insect AQPs. Scale bar represents the number of amino acid substitutions per site. Numbers at the nodes are bootstrap values (only bootstrap values >50 are shown). The sequences are indicated by the initials of the scientific name of the species, followed by the accession number and, in parentheses, the acronym commonly used, if any. Complete binomial names of the species are indicated in Materials and methods. The PRIP (*Pyrocoelia rufa* integral protein), DRIP (*Drosophila* integral protein) and BIB (neurogenic gene *Drosophila* big brain) nodes are indicated. BgAQP falls into the PRIP node. Also indicated are the aquaglyceroporins (Glp) AQP-Bom2 from *Bombyx mori* and AQP-Gra2 from *Grapholita molesta*, in the node of non-classified AQPs.

appears as the sister group of PRIP, and the BIB cluster appears as the sister group of DRIP+PRIP. The fourth node of unclassified AQPs appears as the sister group of DRIP+PRIP+BIB.

Fig. 2 depicts an amino acid alignment of BgAQP with the four AQPs of the PRIP node that have been functionally characterized: EsAQP1 (Philip et al., 2011), AgAQP1 (Liu et al., 2011), PvAQP1 (Kikawada et al., 2008) and BaAQP1 (Goto et al., 2011). The percentage identity of BgAQP with PvAQP1, AgAQP1, BaAQP1 and EsAQP1, all four from dipteran species, falls between 38% and 41%. All the amino acid sequences show the typical P1–P5 and ar/R residues conserved in water-selective AQPs, but they lack the Cys upstream of the second NPA motif considered to be the mercury-sensitive site of some vertebrate AQPs.

Water and solute permeability of BgAQP expressed in *X. laevis* oocytes

To study whether BgAQP effectively transports water, BgAQP cDNA was ectopically expressed in *X. laevis* oocytes. Forty-eight hours after cRNA microinjection, oocytes were transferred to a hypo-osmotic medium and oocyte swelling was determined. These experiments indicated that the water permeability of oocytes expressing 10 ng BgAQP cRNA was 18-fold higher than that of control (water-injected) oocytes (Fig. 3A). Despite the fact that BgAQP does not show a Cys residue preceding the second NPA motif, pre-incubation of oocytes with 1 mmol l^{-1} $HgCl_2$ significantly reduced (P<0.05) the P_f of BgAQP-expressing oocytes, and this inhibition was partially reversed with the reducing agent β-mercaptoethanol (Fig. 3A).

To investigate whether BgAQP is a water-selective AQP, like other members of the PRIP group of insect AQPs, the glycerol and urea permeability of oocytes expressing BgAQP was analysed by radioactive solute uptake assays. For these experiments, we used oocytes expressing 25 ng BgAQP cRNA, as well as negative and positive control oocytes expressing human AQP1 or AQP3, to determine whether BgAQP was able to transport solutes. The results confirmed that BgAQP-expressing oocytes did not transport glycerol significantly (Fig. 3B). However, urea was incorporated at slightly but significantly (P<0.05) higher levels in oocytes expressing BgAQP than in water-injected oocytes or in oocytes expressing human AQP1 (negative control). These data indicate that BgAQP can transport urea, although in much lower amounts than human AQP3 (positive control) (Fig. 3C).

mRNA expression of BgAQP1 in the ovary during adult development

Although the BgAQP was isolated from ovarian tissue, we were interested in assessing whether it was ovary specific. Thus, we analysed BgAQP mRNA expression by qRT-PCR in the ovary, fat body, muscle, digestive tract, Malpighian tubules and colleterial glands collected from 3 day old adult females. The highest levels of BgAQP mRNA were observed in the ovaries; lower expression was detected in the fat body and muscle tissues, whereas it was almost undetectable in colleterial glands, digestive tract and Malpighian tubules (Fig. 4A).

Next, we studied the expression pattern of BgAQP in the ovary. Total RNA was isolated from pools of four to six ovary pairs collected from animals at selected ages and stages, and mRNA levels were analysed by qRT-PCR. We then determined the expression of BgAQP in the ovaries during the transition from 6th nymphal instar to adult, and thereafter during the 7 days of the first gonadotrophic

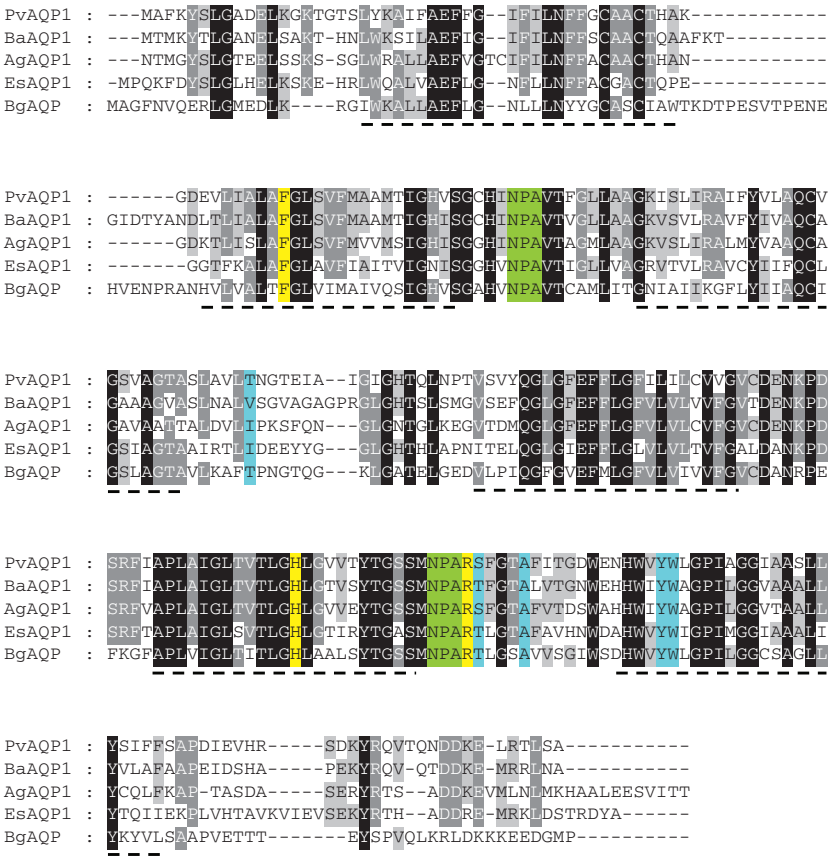

Fig. 2. Amino acid sequence alignment of BgAQP from *B. germanica* with the four AQPs of the insect PRIP node that have been functionally characterized: BaAQP1 from *Belgica antarctica* (AB602340), which transports water but not glycerol or urea (Goto et al., 2011), PvAQP1 from *Polypedilum vanderplanki* (BAF62090.1), which transports water but not glycerol (urea transport was not studied) (Kikawada et al., 2008), and AgAQP1 from *Anopheles gambiae* (XP_319585.4) and EsAQP1 from *Eurosta solidaginis* (FJ489680), which transport water (Liu et al., 2011; Philip et al., 2011). Fully conserved amino acids are shaded in black, whereas conserved substitutions are shaded in grey. The transmembrane domains of BgAQP1 are underlined, and the NPA motifs are highlighted in green. The amino acids typically conserved in water-selective AQPs in the ar/R constriction region (de Groot et al., 2003) and in positions P1–P5 (Froger et al., 1998) are shaded in yellow and blue, respectively.

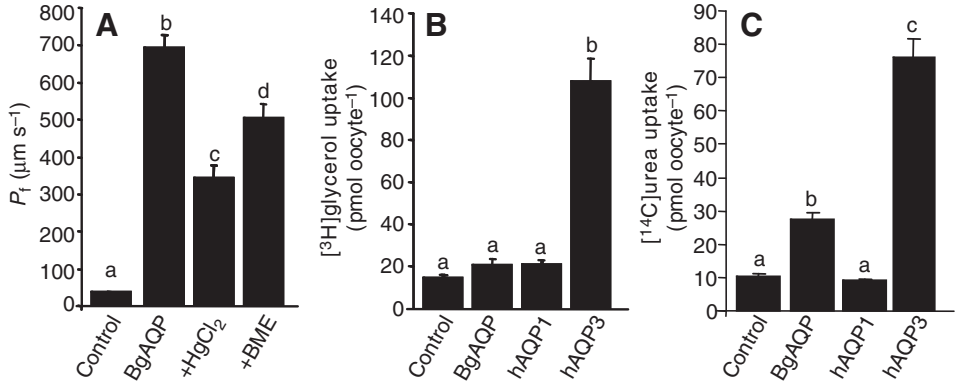

Fig. 3. Water and solute permeability of BgAQP expressed in *X. laevis* oocytes. (A) Osmotic water permeability (P_f) of oocytes injected with water (control) or expressing 10 ng BgAQP cRNA. Water permeability was inhibited with 1 mmol l^{-1} $HgCl_2$ and reversed with 5 mmol l^{-1} β-mercaptoethanol (BME) (*N*=12 oocytes). (B,C) Radioactive glycerol (B) and urea (C) uptake by control oocytes and oocytes expressing 25 ng cRNA encoding BgAQP, human AQP1 (hAQP1) or human AQP3 (hAQP3) (*N*=10–12 oocytes). In each histogram, different letters at the top of the columns indicate significant differences (*t*-test, $P<0.001$). Data are expressed as the mean + s.e.m.

cycle of the adult. The results (Fig. 4B) showed that BgAQP transcript levels are moderate (*ca*. 35 copies of BgAQP per 1000 copies of BgActin-5c) during the last 2 days of the 6th nymphal instar. They then increase *ca*. 2-fold in freshly emerged adults, and decrease thereafter (5–20 copies of BgAQP per 1000 copies of BgActin-5c) between day 1 and day 7, in the stage of late chorion formation (D7LC) (Fig. 4B).

In order to study whether BgAQP could play a role in the ovary under conditions of water stress, we conducted a water-deprivation experiment. Adult *B. germanica* females were provided with food and water *ad libitum* during the first 3 days of adult life, and water was then removed. Under these conditions, the specimens underwent basal oocyte resorption from day 5. Using this experimental design, we measured ovarian BgAQP mRNA levels by qRT-PCR on days 4, 5, 6 and 7 of the first gonadotrophic cycle in control and water-stressed adult specimens. Although the results (Fig. 4C) showed a slight increase of BgAQP1 mRNA levels in water-stressed specimens at days 4 and 6, the differences were not statistically significant.

RNAi experiments

To investigate the role of BgAQP, the expression of BgAQP was silenced by RNAi and the phenotype determined. For these experiments, dsBgAQP was injected into freshly emerged 6th instar female nymphs, and controls were injected with dsMock in the same conditions. The objective was to deplete the peak of BgAQP mRNA occurring in ovaries of freshly emerged adults (Fig. 4B), which might be functionally important, for example to avoid desiccation immediately after moulting. Just after the imaginal moult, BgAQP mRNA levels in dsBgAQP-treated specimens were 12.19±1.22 copies per 1000 copies of BgActin-5c, whereas in dsMock-treated specimens they were 55.34±8.17 copies per 1000 copies of BgActin-5c (Fig. 4D), which indicates that BgAQP mRNA levels were reduced *ca*. 80% by the RNAi. Statistically, according to REST-2008 (Pfaffl et al., 2002), BgAQP was down-regulated in ovaries from dsBgAQP-treated specimens by a mean factor of 0.223 ($P<0.0001$). The duration of the 6th nymphal instar was 8 days in both dsBgAQP-treated specimens and controls, and the imaginal moult proceeded normally. After the moult, we added one mature male per female and studied the first reproductive cycle of the females. The number of days until the formation of the first ootheca was 7 in both treated and control specimens, and most of the mated females formed the ootheca correctly (10 out of 11 in dsBgAQP treated and 7 out of 7 in controls). All ootheca were viable, and the duration of embryogenesis was similar in control and treated specimens, *ca*. 18 days. The number of nymphs hatched per ootheca was 40.71±4.07 in controls (*N*=7) and 36.36±9.24 in treated specimens (*N*=10), differences that were not statistically significant.

DISCUSSION

We have isolated and functionally characterized a novel AQP from the ovary of the cockroach *B. germanica*, which has been named BgAQP. Its deduced amino acid sequence shows the characteristic structural features of AQPs. BgAQP has the ar/R constriction and P1–P5 residues typically conserved in water-specific AQPs (Beitz et al., 2006; Froger et al., 1998). Accordingly, BgAQP effectively transported water when expressed in *X. laevis* oocytes, and this transport was inhibited by mercury chloride ($HgCl_2$) and recovered with β-mercaptoethanol, as occurs for other AQPs (Yukutake et al., 2008). Site-directed mutations on human AQP1 have revealed that the Cys^{189}, located three amino acids upstream of the second NPA in loop E, is the mercury-sensitive site (Preston et al., 1993). However, it has been shown that the absence of Cys^{198} does not prevent inhibition of water flux by mercury (Daniels et al., 1996; Tingaud-Sequeira et al., 2008; Yukutake et al., 2008), which implies that sensitivity of AQPs to mercurial compounds may involve other residues in addition to Cys^{189}. BgAQP lacks a Cys residue near the second NPA box, but it has a Cys residue a short distance downstream of the first NPA in loop B (Cys^{98}). This residue could be a good candidate as the site for mercurial inhibition in BgAQP as it shows a spatial position similar to Cys^{189} in AQP1. Other insect AQPs lacking a Cys residue on loop E, such as PvAQP1 and EsAQP1, are also mercury sensitive and, similar to BgAQP, have a candidate Cys in loop B (Duchesne et al., 2003; Kikawada et al., 2008; Philip et al., 2011).

In our study, radioactive solute uptake assays showed that BgAQP is not permeable to glycerol but is able to transport low amounts of urea. To date, two insect AQPs from lepidopteran larvae have been found to show glycerol and urea uptake: AQP-Bom2 and AQP-Gra2, which have been classified as typical aquaglyceroporins (Kataoka et al., 2009a; Kataoka et al., 2009b). BgAQP cannot be classified as an aquaglyceroporin because it does not transport glycerol, does not show the residues in the ar/R constriction region conserved in aquaglyceroporins, and is phylogenetically distant from AQP-Bom2 and AQP-Gra2. Our data therefore indicate that BgAQP is the first reported insect AQP from the PRIP group that shows water and urea permeability. This feature has only been described so far for some teleost AQP paralogues related to mammalian AQP8 (Tingaud-Sequeira et al., 2010), which is water and ammonia permeable (Litman et al., 2009). It is unknown whether the structural basis of BgAQP water and urea permeability, while excluding

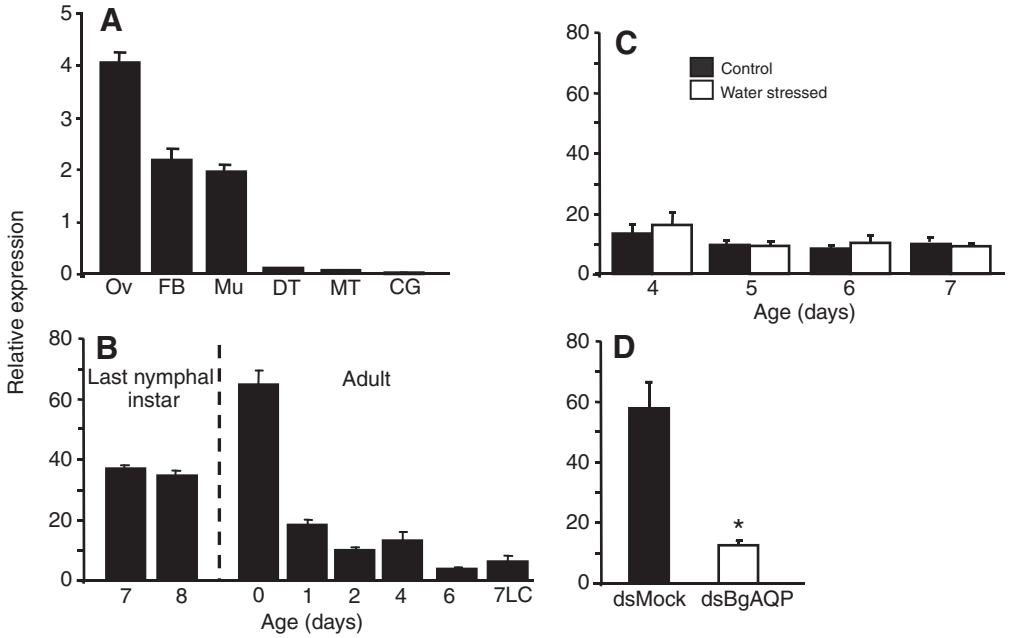

Fig. 4. Expression of BgAQP. (A) Expression in different tissues from 3 day old females (Ov, ovary; FB, fat body; Mu, muscle; DT, digestive tract; MT, Malpighian tubules; CG, colleterial glands). (B) Expression in the ovary during the last 2 days of 6th nymphal instar (days 7 and 8), and during the first gonadotrophic cycle (days 0 to 7LC; LC, late choriogenesis stage). (C) Expression in the ovary of water-stressed females. Females were water deprived on day 3 of adult age, and ovaries were dissected on days 4, 5, 6 or 7, in order to measure BgAQP mRNA levels. Control females were maintained with water *ad libitum*. (D) Expression in dsMock- and dsBgAQP-treated specimens in RNAi experiments. The asterisk indicates that the difference between the two is statistically significant (P<0.0001). Treatments were carried out on freshly emerged 6th (last) instar nymphs, and measurements were taken from freshly emerged adults. Data represent the number of copies per 1000 copies of BgActin-5c, and are expressed as the mean + s.e.m. (N=3).

glycerol, is the same as for teleost AQP8 (Cerdà and Finn, 2010; Tingaud-Sequeira et al., 2010). Nevertheless, the permeability of BgAQP to urea may be physiologically relevant because a metabolic complementation for nitrogen metabolism appears to exist between *B. germanica* and their endosymbiont *B. cuenoti* through the combination of a urea cycle (host) and urease activity (endosymbiont) (Lopez-Sanchez et al., 2009).

The phylogenetic analyses reported by Campbell and colleagues (Campbell et al., 2008), and subsequently by Mathew and colleagues (Mathew et al., 2011), grouped insect AQPs into four groups: DRIP, PRIP, BIB and non-classified AQPs, the last being the sister group of the other three. Parallel studies carried out by Kambara and colleagues (Kambara et al., 2009), and more recently by Goto and colleagues (Goto et al., 2011), resulted in a tree with a topology similar to that reported by Campbell and colleagues (Campbell et al., 2008), although the main nodes were not nominated but simply numbered. However, the PRIP and DRIP nodes of Campbell et al. (Campbell et al., 2008) are recovered in 'Group 1' of Kambara et al. (Kambara et al., 2009) and Goto et al. (Goto et al., 2011). The tree obtained in our study shows the same topology as in these studies, and consistently clusters the BgAQP sequence into the PRIP node. This node appears functionally heterogeneous given that it contains a member that transports water and urea, BgAQP, and other members that are apparently water selective, namely EsAQP1 (Philip et al., 2011), AgAQP1 (Liu et al., 2011), PvAQP1 (Kikawada et al., 2008) and BaAQP1 (Goto et al., 2011). However, the ability of PvAQP1 and AgAQP1 to transport urea has not been investigated (Kikawada et al., 2008; Liu et al., 2011), and other PRIP members have not been functionally studied at all. Therefore, it remains to be determined whether, like BgAQP, other members of this node can transport urea.

Expression analyses indicated that BgAQP mRNA accumulated in fat body, muscle and ovarian tissues, although the highest transcript levels were observed in the ovary. Another AQP primarily expressed in the ovary has been described in the American dog tick, *Dermacentor variabilis* (Holmes et al., 2008), and it has been speculated that this may function in lipid metabolism and/or water transport. However, no experimental studies have been carried out with this AQP, beyond functional expression in *X. laevis* oocytes. In the yellow fever mosquito *A. aegypti*, six AQPs have been characterized, and one of them, AaAQP2, is strongly expressed in ovaries (as well as in the Malpighian tubules and the midgut) (Drake et al., 2010). Nevertheless, specific knockdown of AaAQP2 through RNAi, although significantly decreasing the corresponding transcript levels, did not give any noticeable phenotype (Drake et al., 2010). In teleosts, a functional AQP1-related water channel has been described in oocytes where it plays a role during oocyte hydration prior to ovulation (Fabra et al., 2005; Zapater et al., 2011). During vitellogenesis, basal oocytes of *B. germanica* increase in size exponentially as a result of the incorporation of yolk precursors and water (Belles et al., 1987; Ciudad et al., 2006; Martín et al., 1995), and AQPs may be involved in oocyte water balance during this process. Concerning the expression pattern in the ovary, BgAQP mRNA levels show a peak in freshly emerged adult females, which suggests that most of the BgAQP mRNA necessary for the first reproductive cycle is produced just after the imaginal moult, and then their translation is regulated according to protein requirement.

To investigate the functions of BgAQP in the ovary of *B. germanica*, we monitored its expression in water-stressed specimens. The hypothesis was that water deprivation would modify the

expression of BgAQP in the ovary, as one the earliest consequences of water stress in *B. germanica* is the resorption of the oocytes. However, despite the fact that ovaries from water-stressed specimens started basal oocyte resorption 48 h after water deprivation, no significant differences were observed in the levels of BgAQP mRNA in the ovary between control and water-stressed specimens. AQPs are regulated post-translationally by phosphorylation-dependent gating and especially by trafficking of the protein between the plasma membrane and the intracellular storage vesicle (Törnroth-Horsefield et al., 2010); thus, the effects of water stress on BgAQP may not be evident at the mRNA level.

As a further approach to investigating the role of BgAQP in the ovary, we performed RNAi experiments. *Blattella germanica* is very sensitive to RNAi (Belles, 2010), and expression of membrane-associated proteins has been successfully silenced (Ciudad et al., 2006). The timing of the treatment was designed to deplete the peak of ovarian BgAQP mRNA that occurs in freshly emerged adults, and it was efficiently depleted (by 80%) by our RNAi experiments. However, no phenotypic differences were observed. These results are reminiscent of those obtained with *A. aegypti* (see above). The most parsimonious explanation for these results is that there must be other ovarian AQPs in *B. germanica* with functions overlapping those of BgAQP that were not affected by our RNAi experiments. Indeed, an insect as successful as *B. germanica*, arguably well adapted to xeric environments (Appel, 1995), is likely to have robust and redundant mechanisms to regulate water balance.

ACKNOWLEDGEMENTS

We are grateful to Javier Igea for his help with the phylogenetic analyses. Thanks are also due to David L. Denlinger and Shin G. Goto for providing us with the sequence of BaAQP1 that was used in our phylogenetic analyses.

FUNDING

Financial support for this work was provided by the Spanish Ministry of Science and Innovation [grant number BFU2008-00484 to M.-D.P., grant number CGL2008-03517/BOS to X.B., grant number AGL2010-15597 to J.C.]; and Generalitat de Catalunya [grant number 2005 SGR 00053]. Laboratorio Internacional de Cambio Global (LINC-Global) is gratefully acknowledged. A.H. received a pre-doctoral research grant (JAE-LINCG program) from Consejo Superior de Investigaciones Científicas (CSIC). F.C. was supported by a postdoctoral fellowship from Juan de la Cierva Programme (Spanish Ministry of Science and Innovation).

REFERENCES

Appel, A. G. (1995). *Blattella* and related species. In *Understanding and Controlling the German Cockroach* (ed. M. K. Rust, J. M. Owens and D. A. Reierson), pp. 1-20. New York: Oxford University Press.

Bates, P. A., Kelley, L. A., MacCallum, R. M. and Sternberg, M. J. (2001). Enhancement of protein modeling by human intervention in applying the automatic programs 3D-JIGSAW and 3D-PSSM. *Proteins* **Suppl. 5**, 39-46.

Beitz, E., Wu, B., Holm, L. M., Schultz, J. E. and Zeuthen, T. (2006). Point mutations in the aromatic/arginine region in aquaporin 1 allow passage of urea, glycerol, ammonia, and protons. *Proc. Natl. Acad. Sci. USA* **103**, 269-274.

Belles, X. (2010). Beyond *Drosophila*: RNAi *in vivo* and functional genomics in insects. *Annu. Rev. Entomol.* **55**, 111-128.

Belles, X., Casas, J., Messeguer, A. and Piulachs, M. D. (1987). *In vitro* biosynthesis of JH III by the corpora allata of *Blattella germanica* (L.) adult females. *Insect Biochem.* **17**, 1007-1010.

Blom, N., Gammeltoft, S. and Brunak, S. (1999). Sequence and structure-based prediction of eukaryotic protein phosphorylation sites. *J. Mol. Biol.* **294**, 1351-1362.

Blom, N., Sicheritz-Ponten, T., Gupta, R., Gammeltoft, S. and Brunak, S. (2004). Prediction of post-translational glycosylation and phosphorylation of proteins from the amino acid sequence. *Proteomics* **4**, 1633-1649.

Büning, J. (1994). *The Insect Ovary. Ultrastructure, Previtellogenic Growth and Evolution.* London: Chapman & Hall.

Campbell, E. M., Ball, A., Hoppler, S. and Bowman, A. S. (2008). Invertebrate aquaporins: a review. *J. Comp. Physiol. B* **178**, 935-955.

Castresana, J. (2000). Selection of conserved blocks from multiple alignments for their use in phylogenetic analysis. *Mol. Biol. Evol.* **17**, 540-552.

Cerdà, J. and Finn, R. N. (2010). Piscine aquaporins: an overview of recent advances. *J. Exp. Zool. A Ecol. Genet. Physiol.* **313**, 623-650.

Ciudad, L., Piulachs, M. D. and Belles, X. (2006). Systemic RNAi of the cockroach vitellogenin receptor results in a phenotype similar to that of the *Drosophila* yolkless mutant. *FEBS J.* **273**, 325-335.

Daniels, M. J., Chaumont, F., Mirkov, T. E. and Chrispeels, M. J. (1996). Characterization of a new vacuolar membrane aquaporin sensitive to mercury at a unique site. *Plant Cell* **8**, 587-599.

de Groot, B. L., Frigato, T., Helms, V. and Grubmuller, H. (2003). The mechanism of proton exclusion in the aquaporin-1 water channel. *J. Mol. Biol.* **333**, 279-293.

Deen, P. M., Verdijk, M. A., Knoers, N. V., Wieringa, B., Monnens, L. A., van Os, C. H. and van Oost, B. A. (1994). Requirement of human renal water channel aquaporin-2 for vasopressin-dependent concentration of urine. *Science* **264**, 92-95.

Drake, L. L., Boudko, D. Y., Marinotti, O., Carpenter, V. K., Dawe, A. L. and Hansen, I. A. (2010). The Aquaporin gene family of the yellow fever mosquito, *Aedes aegypti*. *PLoS ONE* **5**, e15578.

Duchesne, L., Hubert, J. F., Verbavatz, J. M., Thomas, D. and Pietrantonio, P. V. (2003). Mosquito (*Aedes aegypti*) aquaporin, present in tracheolar cells, transports water, not glycerol, and forms orthogonal arrays in *Xenopus* oocyte membranes. *Eur. J. Biochem.* **270**, 422-429.

Echevarria, M., Ramirez-Lorca, R., Hernandez, C. S., Gutierrez, A., Mendez-Ferrer, S., Gonzalez, E., Toledo-Aral, J. J., Ilundain, A. A. and Whittembury, G. (2001). Identification of a new water channel (Rp-MIP) in the Malpighian tubules of the insect *Rhodnius prolixus*. *Pflugers Arch.* **442**, 27-34.

Fabra, M., Raldua, D., Power, D. M., Deen, P. M. and Cerdà, J. (2005). Marine fish egg hydration is aquaporin-mediated. *Science* **307**, 545.

Froger, A., Tallur, B., Thomas, D. and Delamarche, C. (1998). Prediction of functional residues in water channels and related proteins. *Protein Sci.* **7**, 1458-1468.

Giorgi, F. and Nordin, J. H. (1994). Structure of yolk granules in oocytes and eggs of *Blattella germanica* and their interaction with vitellophages and endosymbiotic bacteria during granule degradation. *J. Insect Physiol.* **40**, 1077-1092.

Gomes, D., Agasse, A., Thiebaud, P., Delrot, S., Geros, H. and Chaumont, F. (2009). Aquaporins are multifunctional water and solute transporters highly divergent in living organisms. *Biochim. Biophys. Acta* **1788**, 1213-1228.

Goto, S. G., Philip, B. N., Teets, N. M., Kawarasaki, Y., Lee, R. E., Jr and Denlinger, D. L. (2011). Functional characterization of an aquaporin in the Antarctic midge *Belgica antarctica*. *J. Insect Physiol.* **57**, 1106-1114.

Guindon, S. and Gascuel, O. (2003). A simple, fast, and accurate algorithm to estimate large phylogenies by maximum likelihood. *Syst. Biol.* **52**, 696-704.

Hirano, Y., Okimoto, N., Kadohira, I., Suematsu, M., Yasuoka, K. and Yasui, M. (2010). Molecular mechanisms of how mercury inhibits water permeation through aquaporin-1: understanding by molecular dynamics simulation. *Biophys. J.* **98**, 1512-1519.

Holmes, S. P., Li, D., Ceraul, S. M. and Azad, A. F. (2008). An aquaporin-like protein from the ovaries and gut of American dog tick (Acari: Ixodidae). *J. Med. Entomol.* **45**, 68-74.

Jung, J. S., Preston, G. M., Smith, B. L., Guggino, W. B. and Agre, P. (1994). Molecular structure of the water channel through aquaporin CHIP. The hourglass model. *J. Biol. Chem.* **269**, 14648-14654.

Kambara, K., Takematsu, Y., Azuma, M. and Kobayashi, J. (2009). cDNA cloning of aquaporin gene expressed in the digestive tract of the Formosan subterranean termite, *Coptotermes formosanus* Shiraki (Isoptera: Rhinotermitidae). *Appl. Entomol. Zool.* **44**, 315-321.

Kataoka, N., Miyake, S. and Azuma, M. (2009a). Aquaporin and aquaglyceroporin in silkworms, differently expressed in the hindgut and midgut of *Bombyx mori*. *Insect Mol. Biol.* **18**, 303-314.

Kataoka, N., Miyake, S. and Azuma, M. (2009b). Molecular characterization of aquaporin and aquaglyceroporin in the alimentary canal of *Grapholita molesta* (the oriental fruit moth) – comparison with *Bombyx mori* aquaporins. *J. Insect Biotechnol. Sericol.* **78**, 2_81-2_90.

Kaufmann, N., Mathai, J. C., Hill, W. G., Dow, J. A., Zeidel, M. L. and Brodsky, J. L. (2005). Developmental expression and biophysical characterization of a *Drosophila melanogaster* aquaporin. *Am. J. Physiol. Cell Physiol.* **289**, C397-C407.

Kikawada, T., Saito, A., Kanamori, Y., Fujita, M., Snigorska, K., Watanabe, M. and Okuda, T. (2008). Dehydration-inducible changes in expression of two aquaporins in the sleeping chironomid, *Polypedilum vanderplanki*. *Biochim. Biophys. Acta* **1778**, 514-520.

King, L. S., Kozono, D. and Agre, P. (2004). From structure to disease: the evolving tale of aquaporin biology. *Nat. Rev. Mol. Cell Biol.* **5**, 687-698.

Krogh, A., Larsson, B., von Heijne, G. and Sonnhammer, E. L. (2001). Predicting transmembrane protein topology with a hidden Markov model: application to complete genomes. *J. Mol. Biol.* **305**, 567-580.

Le Caherec, F., Deschamps, S., Delamarche, C., Pellerin, I., Bonnec, G., Guillam, M. T., Thomas, D., Gouranton, J. and Hubert, J. F. (1996). Molecular cloning and characterization of an insect aquaporin functional comparison with aquaporin 1. *Eur. J. Biochem.* **241**, 707-715.

Letunic, I., Doerks, T. and Bork, P. (2009). SMART 6, recent updates and new developments. *Nucleic Acids Res.* **37**, D229-D232.

Litman, T., Sogaard, R. and Zeuthen, T. (2009). Ammonia and urea permeability of mammalian aquaporins. *Handb. Exp. Pharmacol.* **190**, 327-358.

Liu, K., Tsujimoto, H., Cha, S. J., Agre, P. and Rasgon, J. L. (2011). Aquaporin water channel AgAQP1 in the malaria vector mosquito *Anopheles gambiae* during blood feeding and humidity adaptation. *Proc. Natl. Acad. Sci. USA* **108**, 6062-6066.

Lopez-Sanchez, M. J., Neef, A., Pereto, J., Patino-Navarrete, R., Pignatelli, M., Latorre, A. and Moya, A. (2009). Evolutionary convergence and nitrogen metabolism in *Blattabacterium* strain Bge, primary endosymbiont of the cockroach *Blattella germanica*. *PLoS Genet.* **5**, e1000721.

Martín, D., Piulachs, M. D. and Bellés, X. (1995). Patterns of haemolymph vitellogenin and ovarian vitellin in the German cockroach, and the role of juvenile hormone. *Physiol. Entomol.* **20**, 59-65.

Mathew, L. G., Campbell, E. M., Yool, A. J. and Fabrick, J. A. (2011). Identification and characterization of functional aquaporin water channel protein from alimentary tract of whitefly, *Bemisia tabaci*. *Insect Biochem. Mol. Biol.* **41**, 178-190.
Maurel, C., Verdoucq, L., Luu, D. T. and Santoni, V. (2008). Plant aquaporins: membrane channels with multiple integrated functions. *Annu. Rev. Plant Biol.* **59**, 595-624.
Murata, K., Mitsuoka, K., Hirai, T., Walz, T., Agre, P., Heymann, J. B., Engel, A. and Fujiyoshi, Y. (2000). Structural determinants of water permeation through aquaporin-1. *Nature* **407**, 599-605.
Pfaffl, M. W., Horgan, G. W. and Dempfle, L. (2002). Relative expression software tool (REST) for group-wise comparison and statistical analysis of relative expression results in real-time PCR. *Nucleic Acids Res.* **30**, e36.
Philip, B. N., Kiss, A. J. and Lee, R. E., Jr (2011). The protective role of aquaporins in the freeze-tolerant insect *Eurosta solidaginis*: functional characterization and tissue abundance of EsAQP1. *J. Exp. Biol.* **214**, 848-857.
Preston, G. M., Jung, J. S., Guggino, W. B. and Agre, P. (1993). The mercury-sensitive residue at cysteine 189 in the CHIP28 water channel. *J. Biol. Chem.* **268**, 17-20.
Rojek, A., Praetorius, J., Frokiaer, J., Nielsen, S. and Fenton, R. A. (2008). A current view of the mammalian aquaglyceroporins. *Annu. Rev. Physiol.* **70**, 301-327.
Shakesby, A. J., Wallace, I. S., Isaacs, H. V., Pritchard, J., Roberts, D. M. and Douglas, A. E. (2009). A water-specific aquaporin involved in aphid osmoregulation. *Insect Biochem. Mol. Biol.* **39**, 1-10.
Telfer, W. H. (2009). Egg formation in lepidoptera. *J. Insect Sci.* **9**, 1-21.
Tingaud-Sequeira, A., Chauvigné, F., Fabra, M., Lozano, J., Raldua, D. and Cerdà, J. (2008). Structural and functional divergence of two fish aquaporin-1 water channels following teleost-specific gene duplication. *BMC Evol. Biol.* **8**, 259.
Tingaud-Sequeira, A., Calusinska, M., Finn, R. N., Chauvigné, F., Lozano, J. and Cerdà, J. (2010). The zebrafish genome encodes the largest vertebrate repertoire of functional aquaporins with dual paralogy and substrate specificities similar to mammals. *BMC Evol. Biol.* **10**, 38.
Törnroth-Horsefield, S., Hedfalk, K., Fischer, G., Lindkvist-Petersson, K. and Neutze, R. (2010). Structural insights into eukaryotic aquaporin regulation. *FEBS Lett.* **584**, 2580-2588.
Yanochko, G. M. and Yool, A. J. (2002). Regulated cationic channel function in *Xenopus* oocytes expressing *Drosophila* big brain. *J. Neurosci.* **22**, 2530-2540.
Yukutake, Y., Tsuji, S., Hirano, Y., Adachi, T., Takahashi, T., Fujihara, K., Agre, P., Yasui, M. and Suematsu, M. (2008). Mercury chloride decreases the water permeability of aquaporin-4-reconstituted proteoliposomes. *Biol. Cell* **100**, 355-363.
Zapater, C., Chauvigné, F., Norberg, B., Finn, R. N. and Cerdà, J. (2011). Dual neofunctionalization of a rapidly evolving aquaporin-1 paralog reveals constrained and relaxed traits controlling channel function during meiosis resumption in marine teleosts. *Mol. Biol. Evol.* (Epub ahead of print).
Zardoya, R. (2005). Phylogeny and evolution of the major intrinsic protein family. *Biol. Cell* **97**, 397-414.